JOURNAL OF PROPULSION AND POWER
Vol. 22, No. 6, November–December 2006

Experimental Characterization of Cavitation Instabilities in a Two-Bladed Axial Inducer

Angelo Cervone,* Cristina Bramanti,† and Emilio Rapposelli‡
ALTA S.p.A., 56121 Ospedaletto, Pisa, Italy
and
Lucio Torre§ and Luca d'Agostino‖
University of Pisa, 56126 Pisa, Italy

DOI: 10.2514/1.19637

The present paper illustrates the main results of an experimental campaign conducted in the Cavitating Pump Rotordynamic Test Facility. The tests were carried out on the FAST2 inducer, a two-bladed axial pump designed and manufactured using the criteria followed for VINCI180 inducer. The transparent inlet section of the facility was instrumented by several piezoelectric pressure transducers located at three axial stations: inducer inlet, outlet and at the middle of the axial chord of the blades. For each axial station at least two transducers were mounted at selected angular spacing, in order to cross correlate their signals for coherence and phase analysis. The most interesting detected instabilities were: a cavitation auto-oscillation at about 5–12 Hz, a high-order cavitation surge at a frequency of about 4.4Ω and a rotating stall at about 0.31Ω. Some experiments were carried out under forced vibration conditions: it was observed that a whirl frequency of about 1 Hz can provide excitation for violent surge-mode oscillations. A "cavitation surge" instability was also observed at higher whirl frequencies.

Nomenclature

f	=	frequency
p_{in}	=	inlet pressure
p_V	=	vapor pressure
Q	=	volumetric flow rate
r_T	=	inducer blade tip radius
S_{XX}	=	power density of the autocorrelated signal
T	=	temperature
α	=	blade tip incidence angle from pressure side (radians)
Δp	=	pressure rise caused by the inducer
ρ	=	density
σ	=	cavitation number
ϕ	=	flow coefficient
ψ	=	head coefficient
Ω	=	rotational speed
ω	=	whirl speed

Introduction

THE design of high power turbopumps for liquid propellant engines is one of the most critical aspects in the work of space rocket engineers. Severe limitations are associated with the realization of high power density, dynamically stable machines capable of meeting the extremely demanding suction, pumping and reliability requirements of space transportation systems (Stripling and Acosta [1]).

Presented as Paper 4451 at the 41st AIAA/ASME/SAE/ASEE Joint Propulsion Conference & Exhibit, Tucson Arizona, 10–13 July 2005; received 23 August 2005; revision received 2 February 2006; accepted for publication 17 February 2006.

*Project Manager; a.cervone@alta-space.com. Member AIAA.
†Project Engineer; currently Post-Doc Fellow, ESA–European Space Research and Technology Centre, Noordwijk, The Netherlands; c.bramanti@alta-space.com.
‡Senior Engineer; e.rapposelli@alta-space.com. Member AIAA.
§M.S. Student, Department of Aerospace Engineering; luciotrr@yahoo.it.
‖Professor, Department of Aerospace Engineering; luca.dagostino@ing.unipi.it.

In typical pumps used in space rocket engines an axial inducer is placed upstream of the centrifugal stages in order to improve the suction performance and reduce the propellant tank pressure and weight. The inducer is one of the most critical components of the turbopump assembly due to the significant cavitation levels occurring in it and, as a consequence, to the development of flow instabilities that can seriously degrade the performance of the machine, or even cause its failure.

A general classification of turbopump flow instabilities is given by Brennen [2], who divides them in three main categories: global oscillations, local oscillations and instabilities caused by radial or rotordynamic forces. Rotating stall and rotating cavitation are considered global oscillations, propagating in the azimuthal direction at angular speeds different from that of the pump (typically subsynchronous for rotating stall and supersynchronous for rotating cavitation). Surge and cavitation auto-oscillations are system instabilities, involving strong longitudinal flow and pressure oscillations of the whole suction line, typically occurring in noncavitating pumps for positive slopes of the head characteristics (surge) and near breakdown conditions in cavitating turbopumps (cavitation auto-oscillations).

The occurrence of rotating cavitation has been extensively reported in the development of most high performance liquid propellant rocket fuel feed systems, including the American Space Shuttle Main Engine, the European Ariane 5 engine, and the LE-7 of the H-II and H-II-A Japanese rockets. Together with surge and auto-oscillations, rotating cavitation is therefore becoming a major concern in modern highly loaded inducers, where both phenomena seemed to be caused by positive values of the pump's mass flow gain factor.

The first comprehensive experimental characterization of rotating cavitation instabilities was reported by Kamijo et al. [3]. They detected the occurrence of slightly supersynchronous rotating cavitation on a three-bladed inducer, leading to strong vibrations of the pump shaft at the same frequency, and suggested a simple modification of the pump housing in order to suppress this instability.

In the following years the research on flow instabilities became more intensive, particularly in Japan. Hashimoto et al. [4] analyzed in detail the influence of the number of blades, carrying out experiments on 3 and 4-bladed inducers. On both inducers they detected the

occurrence of cavitation surge, rotating cavitation and steady asymmetric cavitation. In addition, on the four-bladed inducer they observed a form of alternate blade cavitation, an instability similar to steady asymmetric cavitation and typical of inducers with an even number of blades, where two cavitation cells propagated synchronously at the pump rotational speed. Tsujimoto and his collaborators [5] introduced the use of cross-correlation and phase analysis techniques in the experimental analysis of cavitation instabilities, in order to recognize oscillations of higher order characterized by a certain number of rotating cells. In the United States, Zoladz [6] carried out a series of experiments during the development of the LOX turbopump of the Fastrac engine. An aluminum prototype of the inducer of this turbopump failed due to the strong oscillating stresses caused by cavitation surge and rotating cavitation.

Recently Tsujimoto and Semenov [7] identified in the LE-7 inducers a new high-order cavitation surge (axial) instability, occurring at frequencies as high as 4 to 5 times the pump rotational speed and involving a periodic redistribution of cavitation along the blade channels, with no net change of the total cavitation volume. Contrary to conventional cavitation auto-oscillations, high-order cavitation surge is not therefore a system instability, as also suggested by its much higher frequency. According to the authors, its unforeseen resonance with the first bending mode of the inducer blades was responsible for the fatigue failure of the liquid hydrogen pump inducer of the 8th launch of H-II rocket in November 1999.

A significant amount of work has also been developed for analyzing the various forms of flow instabilities in pumps by theoretical and/or numerical means (Kamijo et al. [8]; Tsujimoto et al. [9]; Tani and Nagashima [10]; d'Agostino and Venturini-Autieri [11,12]).

Recent experiments have been carried out by the authors of the present paper for investigating the influence of thermal cavitation effects on the onset and the development of flow instabilities caused by cavitation. Experiments on a NACA 0015 hydrofoil through the thermal cavitation tunnel showed that both the amplitude and the stability limits of the various cavitation forms and instabilities, observed on the foil, strongly depend on the intensity of thermodynamic effects of the cavitating fluid (Rapposelli et al. [13]). Other experiments, carried out on two axial inducers, showed that thermal cavitation effects have a generally stabilizing effect on the onset of some cavitation-induced instabilities, by significantly reducing the intensity of the pressure oscillations, but do not appreciably change the observed frequency of the instabilities, nor do they introduce significant new oscillation phenomena (Cervone et al. [14]).

The present work illustrates the main results of an experimental activity carried out in the Cavitating Pump Rotordynamic Test Facility on the so-called "FAST2" inducer, a two-bladed axial pump manufactured using the criteria followed for the VINCI180 inducer. Experiments were carried out in order to analyze the noncavitating and cavitating performance of the inducer and to detect the occurrence of flow instabilities in various flow conditions.

Experimental Apparatus

The Cavitating Pump Rotordynamic Test Facility was designed to experimentally characterize turbopumps performance in a wide variety of alternative configurations (axial, radial, or mixed flow, with or without an inducer; Rapposelli et al. [15]). The facility operates in water at temperatures up to 90 deg and is intended as a flexible apparatus readily adaptable to conduct experimental investigations on virtually any kind of fluid dynamic phenomena relevant to high performance turbopumps. The test section (Fig. 1) is equipped with a rotating dynamometer, for the measurement of the forces and moments acting on the impeller, and with a mechanism for adjusting and rotating the eccentricity of the impeller axis in the range 0–2 mm and ± 3000 rpm. The inlet section, made in Plexiglas, is transparent in order to allow for the optical visualization of cavitation on the test inducer. It is known that the inlet section compliance is a factor that could alter the cavitation dynamics and the characteristics of the detected flow instabilities: for this reason tests carried out using different inlet ducts, including metallic (stainless steel) ones, are foreseen in the next future.

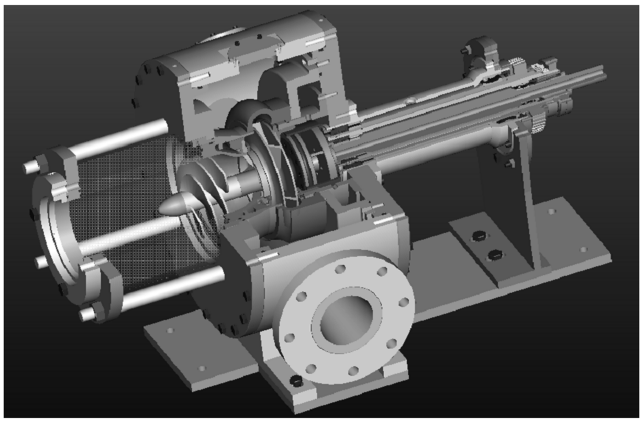

Fig. 1 Cutout drawing of the CPRTF test section.

For the present experimental work the facility was assembled in a simplified configuration without the rotating dynamometer. Some modifications were introduced to the original assembling of the facility in order to facilitate experimentation on the FAST2 inducer, as it will be described in the next section.

The inlet pressure and the pressure rise, necessary for the characterization of the pump performance, were measured by means of an absolute pressure transducer installed upstream of the Plexiglas inlet section (0–1.5 bar operating range, 0.25% precision class) and a pair of redundant differential pressure transducers installed between the inlet and the outlet sections of the test pump (0–100 psid operating range, 0.1% precision class; 0–1 bard operating range, 0.08% precision class).

The pressure fluctuations have been analyzed equipping the inlet section (Fig. 2) with flush-mounted piezoelectric pressure transducers (voltage mode-type, 0.1% class) located at three axial stations: inducer inlet, outlet and at the middle of the axial chord of the blades. In particular, the inlet station was located just before the attachment point of the leading edge of the blades. At each axial station at least two transducers have to be mounted with selected angular spacing, in order to cross-correlate their signals for coherence and phase analysis. As a result, waterfall plots of the power spectral density of the pressure fluctuations can be obtained as functions of the cavitation number $\sigma = (p_{\text{in}} - p_V)/\frac{1}{2}\rho\Omega^2 r_T^2$, in order to identify the presence of instabilities. The axial or azimuthal nature of the detected instabilities (and, in the second case, the number of rotating cells involved) can be determined by means of cross correlation of the pressure signals from different locations. All

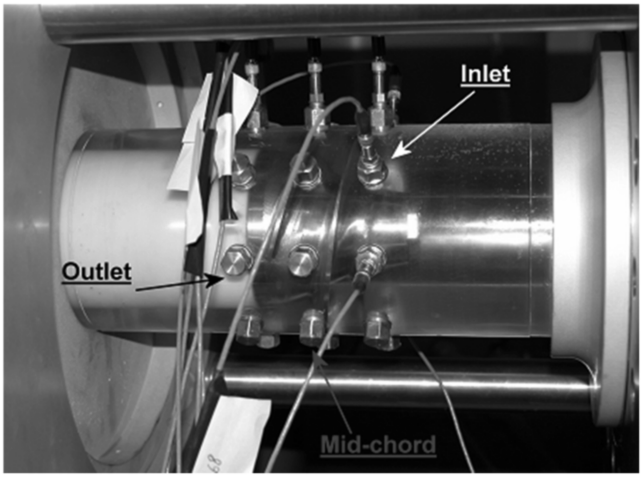

Fig. 2 The inlet section of the facility instrumented with piezoelectric pressure transducers.

Fig. 3 The FAST2 inducer.

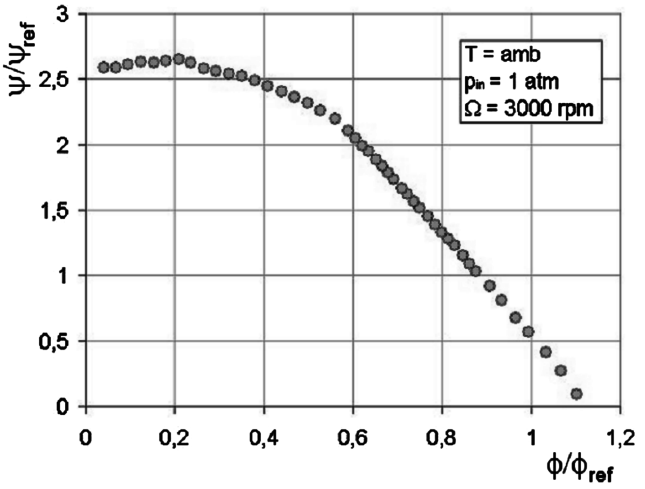

Fig. 4 Noncavitating performance of the FAST2 inducer. Head coefficient ψ/ψ_{ref} plotted as a function of the flow coefficient ϕ/ϕ_{ref} at room water temperature and inlet pressure for $\Omega = 3000$ rpm.

the experiments were carried out maintaining a constant value of the flow coefficient (with a maximum tolerated oscillation equal to $\pm 0.5\%$ of the nominal value) and the pump rotational speed, and gradually reducing the inlet pressure from atmospheric conditions to the minimum allowable value, at a constant rate of about 3 mbar/s. This technique was validated during past experiments and was demonstrated to be accurate and effective for characterizing the nature and spatial configuration of the inducer flow instabilities (Cervone et al. [14]). The accuracy of the electromagnetic flow meters used for the present experiments is $\pm 0.1\%$.

Test Inducer

The FAST2 inducer (Fig. 3) was designed using the criteria followed for VINCI180 inducer and taking into account the results derived from past experience (VULCAIN MK1 and MK2, ATE, VINCI150). Its geometry is characterized by a shallow spiral angle, high-solidity, and low aspect ratio blading.

The FAST2 is a two-bladed stainless steel axial inducer with tip radius $r_T = 41.1$ mm and a profiled, variable-radius hub (15 mm inlet radius, 28 mm outlet radius). The blades are backswept, with variable thickness and nonuniform blade angle. The inlet tip blade angle is 7.38 deg, the outlet tip blade angle is 21.24 deg and the tip solidity is 1.59.

Some modifications were made in the facility test section in order to carry out experiments on the FAST2 inducer in the best possible conditions. In particular, the small dimensions of the inducer led to the necessity of changing the operational parameters of the facility in order to obtain the cavitation numbers required to achieve fully developed cavitation. For this reason a planetary gearbox was installed between the main engine and the pump shaft, giving the possibility of achieving pump rotational speeds up to 10000 rpm. On the other hand, pressure losses in the suction line of the facility were artificially increased, thus obtaining a lower pressure at the inducer inlet, by inserting two packs of stainless steel grids few diameters downstream of the main tank.

The nominal inducer tip clearance during the present experiments was 0.4 mm for the tests without whirling eccentricity, 1.4 mm for whirling eccentricity experiments.

Results and Discussion

Inducer Performance

The noncavitating performance of the FAST2 inducer, in terms of the head coefficient $\psi = \Delta p/\rho\Omega^2 r_T^2$ as a function of the flow coefficient $\phi = Q/\pi\Omega r_T^3$, is shown in Fig. 4. Figure 5 shows the cavitating performance of the inducer in terms of the head coefficient as a function of the cavitation number σ for several values of the flow coefficient. The reference value of the flow coefficient (ϕ_{ref}) has been chosen in order to keep the inducer nominal flow coefficient equal to $0.7\phi_{ref}$. On the other hand, the reference cavitation number (σ_{ref}) is the value of σ for which cavitation breakdown begins at the nominal flow coefficient.

The optical visualization of cavitation inception and development on the inducer showed a peculiar phenomenon. As the flow coefficient increases, cavitation inception has been observed to move from the leading edge of the blades toward their trailing edge. Cavitation develops in the backward direction and, in a less extensive way, on the pressure side of the leading edge. This phenomenon, not typically observed on the inducers used for space rockets applications, is thought to be due to the blade camber of the FAST2 inducer and to the corresponding shape of the pressure profile for lower incidence angles and higher flow coefficients. Conversely, when the flow coefficient decreases cavitation on the trailing edge becomes less extensive and another cavitating region develops at the leading edge. The cavitating region developing from the trailing edge, still present at flow coefficients higher than about 1.2 times the

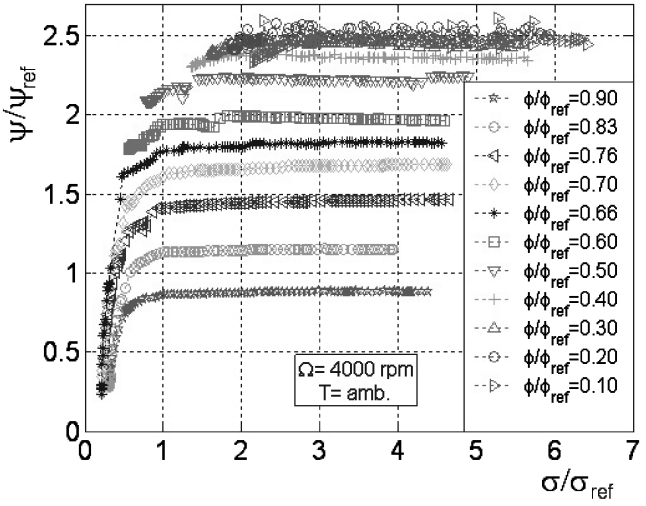

Fig. 5 Cavitating performance of the FAST2 inducer. Head coefficient ψ/ψ_{ref} plotted as a function of the cavitation number σ/σ_{ref} at room water temperature for $\Omega = 4000$ rpm and several values of the flow coefficient ϕ/ϕ_{ref}.

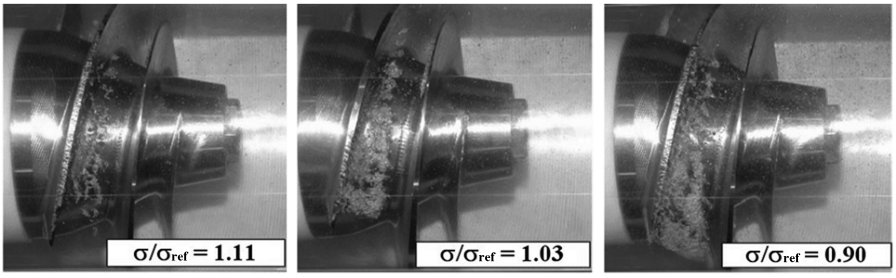

Fig. 6 Cavitation inception and development on the FAST2 inducer for $\phi/\phi_{ref} = 1.05$ at room water temperature, $\Omega = 4000$ rpm and different values of the cavitation number.

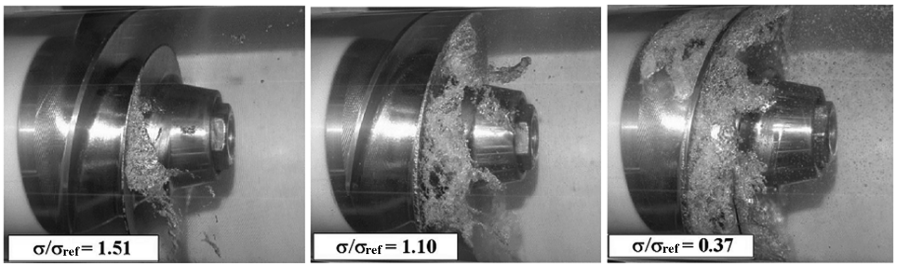

Fig. 7 Cavitation inception and development on the FAST2 inducer for $\phi/\phi_{ref} = 0.7$ at room water temperature, $\Omega = 3500$ rpm and different values of the cavitation number.

nominal one, completely disappears at lower values of the flow coefficient. Figure 6 shows some pictures of trailing edge cavitation on the inducer at high flow coefficients, whereas Fig. 7 presents the appearance of regular leading edge cavitation at lower values of ϕ.

Flow Instabilities

In the experiments for the characterization of the flow instabilities six piezoelectric transducers were mounted at the inducer inlet station at an angular spacing of 45 deg, in order to characterize the occurrence and nature of rotating instabilities. A wide range of flow coefficients were investigated. Figures 8–10 show some typical results for the waterfall plots of the pressure fluctuation spectra measured at the inducer inlet section. "Normalized" pressure oscillations (amplitude of oscillations divided to the mean value of dynamic pressure at inducer tip) have been shown in the waterfall plots as a function of the dimensionless parameter $\sigma/2\alpha$, where α is the blade tip incidence angle from pressure side in radians. In Figs. 11–13 the power spectral density, the phase and the coherence function of the cross correlation between the pressure signals of two transducers placed at 45 deg angular separation in the azimuthal direction are illustrated for some cases of particular interest.

Examination of the spectra shows the occurrence of five forms of instabilities, denoted by frequencies from f_1 to f_5.

1) The frequency f_1 is related to a 0th order (axial) instability. This result can be easily obtained by examination of Fig. 11 because the cross correlation of two pressure signals at the inducer inlet station has 0 deg phase angle with a value of the coherence function practically equal to 1. This instability appears at all values of the flow coefficient and for lower values of σ, when cavitation is completely developed. The frequency is about 5–12 Hz and tends to decrease when the cavitation number is reduced. As a consequence of these characteristics, the instability is probably a typical cavitation auto-oscillation.

2) The frequency f_2 is also related to an axial instability, as clearly shown by the phase and coherence function of the cross correlation presented in Fig. 12. The phenomenon is observed for all the values of ϕ, but tends to become more significant at the higher flow coefficients. Its amplitude tends to decrease at the lower cavitation numbers. The frequency is about 4.4 times the pump rotational

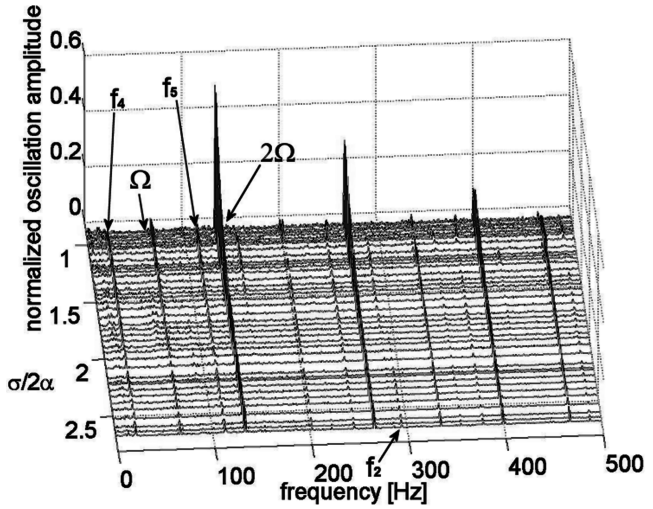

Fig. 8 Waterfall plot of the power spectrum of the normalized inlet pressure fluctuations in the FAST2 inducer at $\phi/\phi_{ref} = 0.1$, 4000 rpm and room water temperature.

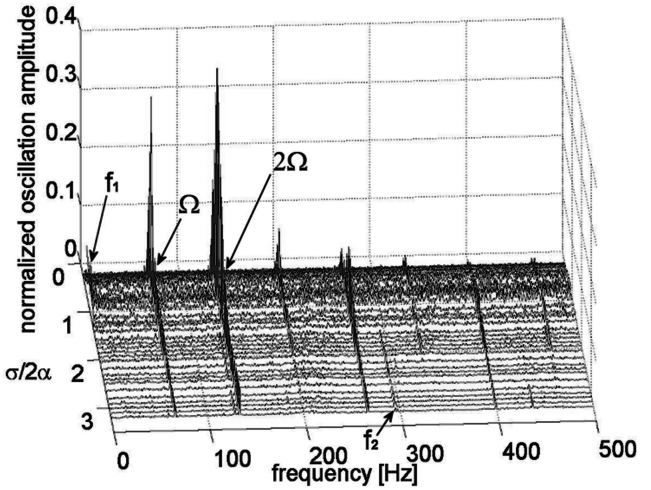

Fig. 9 Waterfall plot of the power spectrum of the normalized inlet pressure fluctuations in the FAST2 inducer at $\phi/\phi_{ref} = 0.7$, 4000 rpm and room water temperature.

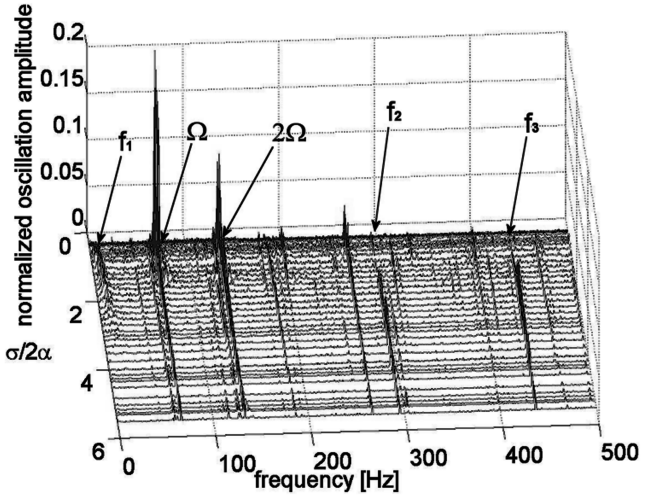

Fig. 10 Waterfall plot of the power spectrum of the normalized inlet pressure fluctuations in the FAST2 inducer at $\phi/\phi_{ref} = 0.9$, 4000 rpm and room water temperature.

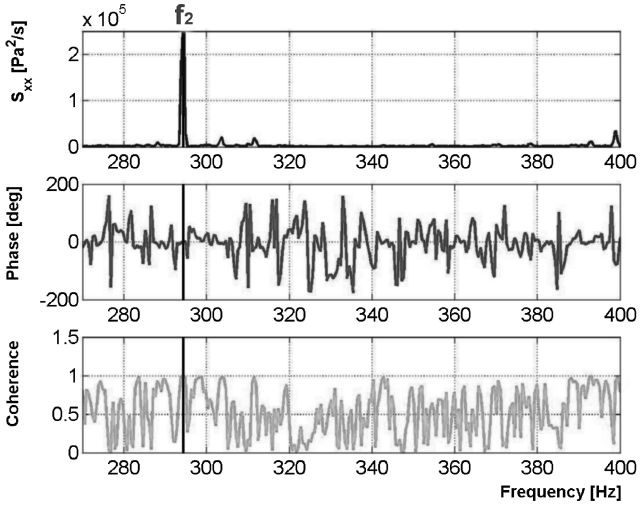

Fig. 12 Power density spectrum, phase of the cross-correlation and coherence function of the pressure signals of two transducers with 45 deg angular separation in the inlet section of the FAST2 inducer ($\phi/\phi_{ref} = 0.9$, $\sigma/\sigma_{ref} = 1.9$, $\Omega = 4000$ rpm).

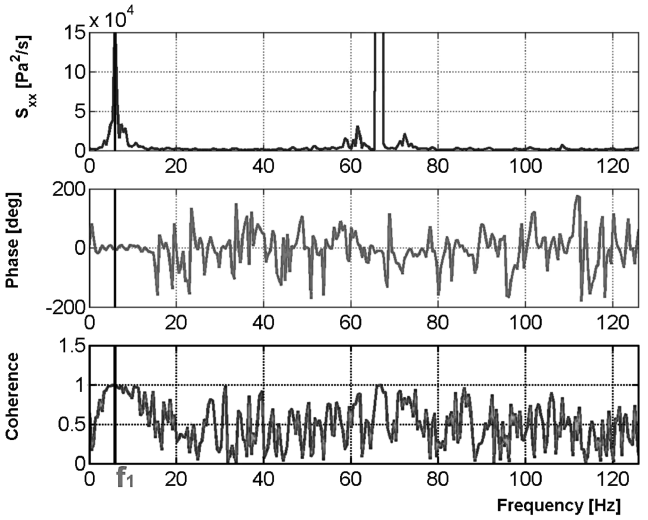

Fig. 11 Power density spectrum, phase of the cross-correlation and coherence function of the pressure signals of two transducers with 45 deg angular separation in the inlet section of the FAST2 inducer ($\phi/\phi_{ref} = 0.9$, $\sigma/\sigma_{ref} = 0.9$, $\Omega = 4000$ rpm).

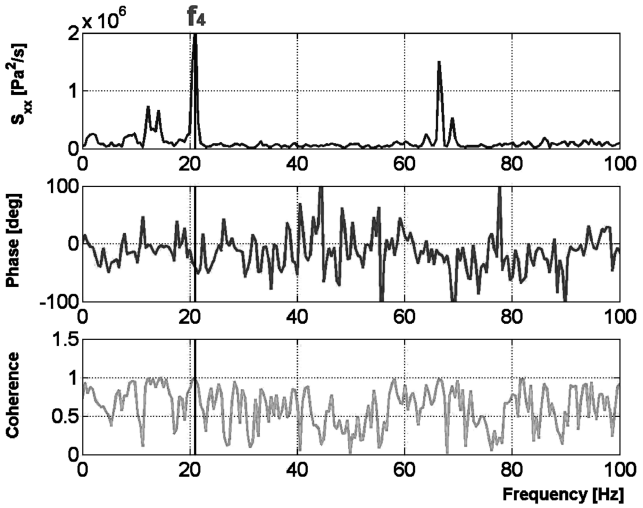

Fig. 13 Power density spectrum, phase of the cross-correlation and coherence function of the pressure signals of two transducers with 45 deg angular separation in the inlet section of the FAST2 inducer ($\phi/\phi_{ref} = 0.1$, $\sigma/\sigma_{ref} = 6.0$, $\Omega = 4000$ rpm).

speed. This instability has characteristics very similar to those of the high-order cavitation surge instability recently observed by Tsujimoto and Semenov [7] on the Japanese LE-7 inducers, whose frequency has been reported to be in the range from 4 to 5 times the pump rotational speed.

3) The frequency f_3 is related to an axial phenomenon, having the same characteristics of the f_2 instability. This finding, together with the strong frequency correlation (the value of f_3 is exactly equal to 1.5 times f_2) leads to the conclusion that the two frequencies are due to the same kind of instability.

4) and 5) The frequencies f_4 and f_5 are related to single-cell rotating instabilities. This conclusion can be drawn by examination of Fig. 13, which shows a phase delay between two transducers at the inducer inlet section equal to their angular spacing, with a value of the coherence function very close to unity. These phenomena appear at the lower values of the flow coefficient, with frequencies $f_4 = 0.31\Omega$ and $f_5 = 1.69\Omega$ symmetrically located above and below the rotating speed. The frequency f_4 tends to decrease slightly (and, correspondingly, f_5 slightly increases) at very low values of the cavitation number. The subsynchronous instability denoted by f_4 can probably be attributed to a form of rotating stall, similar to that reported by Uchiumi et al. [16] during the development of the LE-7A liquid hydrogen pump and probably caused by the occurrence of strong backflow in the inducer inlet. The supersynchronous f_5 frequency is probably related to the same instability phenomenon that moves simultaneously in two directions, the same of the rotating pump (leading to f_5 frequency) and the opposite one (leading to f_4 frequency): this consideration is supported by the strong relationship existing between f_5 and the blade passing frequency 2Ω. Note that a similar form of rotating stall was already detected in the Cavitating Pump Rotordynamic Test Facility during a recent experimentation on a commercial inducer of extremely simple helical geometry [14].

The detection of the rotating frequency Ω in the waterfall plots, in addition to the blade passing frequency 2Ω, is due to the asymmetrical behavior of the flow on the two blades. This was confirmed by optical visualization, which demonstrated the occurrence of cavitation with different shape and size on the two blades.

Finally, in Fig. 9 it can be observed that for $\phi/\phi_{ref} = 0.7$, corresponding to the nominal operating point of the FAST2 inducer, most of the above illustrated flow instabilities are strongly reduced or even suppressed, thus confirming the effectiveness of the pump design.

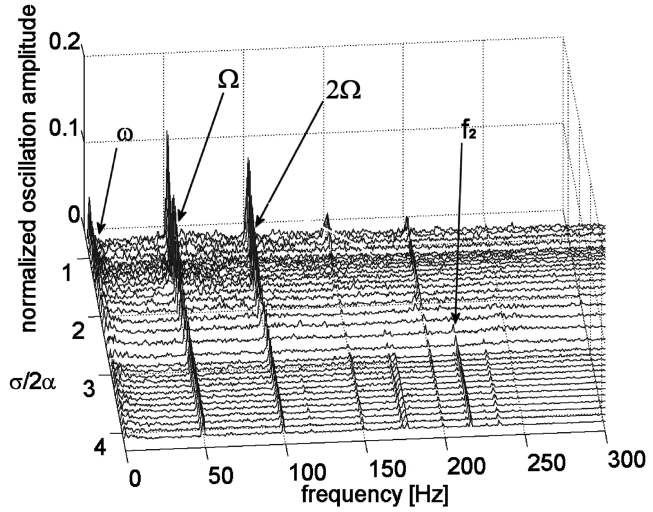

Fig. 14 Waterfall plot of the power spectrum of the normalized inlet pressure fluctuations in the FAST2 inducer under forced vibration conditions at $\phi/\phi_{\text{ref}} = 0.7$, $\Omega = 3000$ rpm, $\omega/\Omega = 0.02$ and room water temperature. The eccentricity of the whirl motion is 0.501 mm (35.8% of the inducer tip clearance).

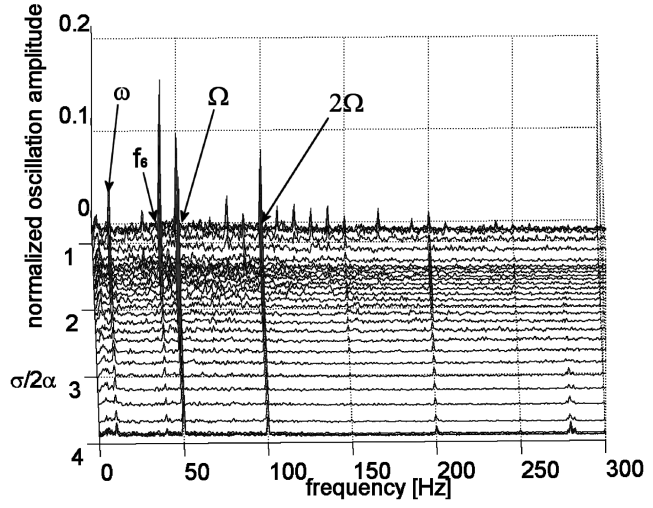

Fig. 15 Waterfall plot of the power spectrum of the normalized inlet pressure fluctuations in the FAST2 inducer under forced vibration conditions at $\phi/\phi_{\text{ref}} = 0.7$, $\Omega = 3000$ rpm, $\omega/\Omega = 0.2$, and room water temperature. The eccentricity of the whirl motion is 0.501 mm (35.8% of the inducer tip clearance).

Whirling Eccentricity Experiments

Two whirling eccentricity experiments were carried out on the FAST2 inducer at 3000 rpm and nominal flow rate ($\phi/\phi_{\text{ref}} = 0.7$). The eccentricity of the rotating whirl motion was set equal to 0.501 mm (i.e., 35.8% of the inducer tip clearance) and the ratio between the whirl speed ω and the inducer rotational speed Ω was 0.02 during the first experiment, 0.2 during the second experiment.

Figures 14 and 15 show the waterfall plots of the normalized pressure fluctuation spectra measured at the inducer inlet section in the two experimental conditions. The most interesting results of these experiments were the following:

1) The whirl frequency ω was clearly detected in both cases, together with the inducer rotating speed Ω . Optical visualization of cavitation on the inducer showed that, for the case $\omega/\Omega = 0.02$ (corresponding to a whirl frequency of 1 Hz), the whirl motion acted as an exciting factor for the development of a violent surge-mode instability having the same frequency. On the other hand, this surge-mode instability was not observed for $\omega/\Omega = 0.2$ because the exciting whirl frequency (10 Hz) is too distant from surge frequency and does not couple with the flow oscillations.

2) For $\omega/\Omega = 0.2$ a new instability was detected, whose frequency is denoted by f_6. Phase and coherence analysis of the cross correlation of pressure signals at the inducer inlet section showed that it is an axial instability, probably a subsynchronous "cavitation surge" at a frequency of about 0.8Ω. Another possible interpretation of this instability is that it is the result of interaction between the attached synchronous cavitation and the rotating whirl component.

3) For $\omega/\Omega = 0.02$ the high-order cavitation surge instability f_2 was still observed at a frequency 4.4Ω, thus indicating that the relatively slow whirl motion imposed to the inducer had little influence on the development of this kind of high-frequency instability.

Conclusions

A set of experiments were carried out in the Cavitating Pump Rotordynamic Test Facility for the characterization of the FAST2 inducer, a two-bladed stainless steel axial pump designed according to the criteria adopted for VINCI180 inducer.

The most interesting conclusions drawn by the experimental activity can be summarized as follows:

1) Optical visualization of cavitation inception and development on the inducer showed that, if the flow coefficient is sufficiently high, cavitation inception moves from the leading edge of the blades toward their trailing edge, developing in the backward direction and, in a less extensive way, on the pressure side of the leading edge. This phenomenon is likely to be due to the blade camber the FAST2 inducer and to the corresponding shape of the pressure profile for lower incidence angles and higher flow coefficients.

2) Several flow instabilities were detected on the inducer, including: a cavitation auto-oscillation, a possible high-order cavitation surge at a frequency of 4.4Ω coupled with another phenomenon having multiple frequency and a rotating stall at a frequency equal to 0.31Ω, moving simultaneously in two directions (the rotational direction of the pump and the opposite one) and leading, as a consequence, to the observation of a couple of frequencies in the power spectrum of the inlet pressure signal, one subsynchronous and the other supersynchronous.

3) Most of the detected flow instabilities were observed to be strongly reduced or even suppressed near the nominal operating point of the inducer, thus confirming the effectiveness of its design.

4) Some experiments were carried out under forced vibration conditions, showing that the whirl motion can excite a violent surge-mode instability if its frequency is about 1 Hz, close to the natural frequency of cavitation surge oscillations. A "cavitation surge" instability with a frequency of 0.8Ω was detected in experiments with whirl frequency equal to 10 Hz.

Acknowledgments

The Cavitating Pump Rotordynamic Test Facility has been funded by the Agenzia Spaziale Italiana under the 1998 and 1999 contracts for fundamental research. The authors would like to thank Mauro Varetti of Avio S.p.A. for his kind assistance and express their gratitude to Mariano Andrenucci and Renzo Lazzeretti of the Dipartimento di Ingegneria Aerospaziale, Università di Pisa, for their constant and friendly encouragement.

References

[1] Stripling, L. B., and Acosta, A. J., "Cavitation in Turbopumps: Part 1," *Journal of Basic Engineering*, Vol. 84, Sept. 1962, pp. 326–338.

[2] Brennen, C. E., *Hydrodynamics of Pumps*, Concepts ETI, Inc. and Oxford University Press, Norwich, VT, 1994.

[3] Kamijo, K., Yoshida, M., and Tsujimoto, Y., "Hydraulic and Mechanical Performance of LE-7 LOX Pump Inducer," *Journal of Propulsion and Power*, Vol. 9, No. 6, 1993, pp. 819–826.

[4] Hashimoto, T., Yoshida, M., Watanabe, M., Kamijo, K., and Tsujimoto, Y., "Experimental Study of Rotating Cavitation of Rocket Propellant Pump Inducers," *Journal of Propulsion and Power*, Vol. 13, No. 4, 1997, pp. 488–494.

[5] Tsujimoto, Y., Yoshida, Y., Maekawa, Y., Watanabe, S., and Hashimoto, T., "Observation of Oscillating Cavitation of an Inducers," *Journal of Fluids Engineering*, Vol. 119, Dec. 1997, pp. 775–781.

[6] Zoladz, T., "Observations on Rotating Cavitation and Cavitation Surge from the Development of the Fastrac Engine Turbopump," *Proceedings of the 36th AIAA/ASME/SAE/ASEE Joint Propulsion Conference, 2000* (unpublished).

[7] Tsujimoto, Y., and Semenov, Y. A., "New Types of Cavitation Instabilities in Inducers," *Proceedings of the 4th International Conference on Launcher Technology, 2002* (unpublished).

[8] Kamijo, K., Shimura, T., and Tsujimoto Y., "Experimental and Analytical Study of Rotating Cavitation," ASME Paper FED-190, 1993, pp. 33–43.

[9] Tsujimoto, Y., Watanabe, S., and Horiguchi, H., "Linear Analyses of Cavitation Instabilities of Hydrofoils and Cascades," *Proceedings of the U.S.–Japan Seminar: Abnormal Flow Phenomena in Turbomachinery, 1998* (unpublished).

[10] Tani, N., and Nagashima, T., "Numerical Analysis of Cryogenic Cavitating Flow on Hydrofoil: Comparison Between Water and Cryogenic Fluids," *Proceedings of the 4th International Conference on Launcher Technology, 2002* (unpublished).

[11] d'Agostino, L., and Venturini-Autieri, M. R., "Three-Dimensional Analysis of Rotordynamic Fluid Forces on Whirling and Cavitating Finite-Length Inducers," *Proceedings of the 9th International Symposium on Transport Phenomena and Dynamics of Rotating Machinery, 2002* (unpublished).

[12] d'Agostino, L., and Venturini-Autieri, M. R., "Rotordynamic Fluid Forces on Whirling and Cavitating Radial Impellers," *Proceedings of the 5th International Symposium on Cavitation, 2003* (unpublished).

[13] Rapposelli, E., Cervone, A., Bramanti, C., and d'Agostino, L., "Thermal Cavitation Experiments on a NACA 0015 Hydrofoil," *Proceedings of the 4th ASME–JSME Joint Fluids Engineering Conference*, 2003.

[14] Cervone, A., Testa, R., Bramanti, C., Rapposelli, E., and d'Agostino, L., "Thermal Effects on Cavitation Instabilities in Helical Inducers," *Journal of Propulsion and Power*, Vol. 21, No. 5, Sept.–Oct. 2005, pp. 893–899.

[15] Rapposelli, E., Cervone, A., and d'Agostino, L., "A New Cavitating Pump Rotordynamic Test Facility," AIAA Paper 2002-4285, 2002.

[16] Uchiumi, M., Kamijo, K., Hirata, K., Konno, A., Hashimoto, T., and Kobayashi, S., "Improvement of Inlet Flow Characteristics of LE-7A Liquid Hydrogen Pump," AIAA Paper 2002-4161, 2002.

T. Wang
Associate Editor